Giant magnetoimpedance and domain structure in FeCuNbSiB films and sandwiched films

Shu-qin Xiao, Yi-hua Liu, Shi-shen Yan, You-yong Dai, Lin Zhang, and Liang-mo Mei
Department of Physics, Shandong University, Jinan 250100, People's Republic of China
(Received 13 July 1999)

Longitudinal and transverse giant magnetoimpedance (GMI) effects are studied in FeCuNbSiB and FeCuNbSiB/Cu/FeCuNbSiB films. In regard to as-deposited single layer films, hardly any GMI effect can be detected, while for as-deposited sandwiched films, the maximum GMI ratios of 32% and 11% are obtained in longitudinal and transverse fields, respectively. After annealing, the maximum GMI ratios of 18% and 14% are obtained for the single-layer films in longitudinal and transverse cases, while for the sandwiched films, the maximum GMI ratios are 67% and 80% in longitudinal and transverse cases, respectively. A giant magnetoinductance ratio as large as 1733% is obtained in annealed sandwiched films at a low frequency of 100 kHz. In order to know the relation between GMI effect and magnetic properties of the samples, the domain structures are observed by the Kerr effect.

INTRODUCTION

The effect of giant magnetoimpedance (GMI) is of both scientific and technological interest, associated with the effect itself and with its potential applications in micromagnetic sensors and magnetic heads for recording. The effect has been studied first for the Co-based amorphous wires having a slightly negative magnetostriction of the order of -10^{-7},[1–5] and recently the study has expanded to the Fe-based amorphous or nanocrystalline wires or ribbons[6–9] and many other soft magnetic materials of geometries, especially to the films (including single-layer and multilayered films).[10–14]

The origin of GMI lies in classical electromagnetism.[3,5,15,16] In a uniform film, the GMI effect is based on the impedance dependence on the skin depth, which is a function of a transverse permeability. The transverse permeability can be controlled with an external applied field. Consequently, the GMI effect originates from the transverse permeability, more specifically from the field dependence on transverse permeability. All mechanisms that influence the magnetization processes of the materials contribute to the GMI effects.[17] In the case of wires or single-layer films, the impedance in a linear approximation can be calculated for any frequency.[18,19] At high frequencies where the skin effect is sufficiently strong so that $d/\delta \gg 1$ ($2d$ is the cross-section size of the samples and δ is the penetration depth), Z is expressed in a simple general way as[15]

$$Z = R_{\mathrm{dc}} \frac{d}{\sqrt{8\pi\sigma\omega}} (\sqrt{\mu_R} - j\sqrt{\mu_L}),$$

$$\mu_R = |\mu_t| + \mu_t'', \quad \mu_L = |\mu_t| - \mu_t'', \tag{1}$$

where R_{dc} is the direct current (dc) resistance, σ is the conductivity, ω is the ac current angular frequency, μ_t is the effective transverse permeability, and μ_t'' is the imaginary value of μ_t. It follows from Eq. (1) that at high frequencies both the resistance and reactance components of Z strongly depend on the transverse permeability. Consequently, the GMI effect in single-layer films can be observed at higher frequencies.[14] Recently, it has been shown that the GMI effect can occur in sandwiched structures of $F/M/F$,[12,13] where F stands for a soft magnetic film and M for a nonmagnetic layer with high conductivity. The GMI effect in these structures appears to be much stronger compared with that in ferromagnetic single-layer films with the same thickness. This is because the ac magnetic flux loop is closed and there is a weak influence of stray magnetic field in sandwiched structures. The condition of a strong skin effect for GMI effect is not required in a sandwiched structure. If the sandwich width is sufficiently large, the leakage of the magnetic flux induced by the current can be neglected.[20] Then, the solution of the impedance equation for three-layered films infinitely extending in two directions can be used. Its low-frequency expansion leads to the following: for $d_c\sigma_c/2 \gg d_m\sigma_m$ the inductive term proportional to μ_e can give the main contribution to Z, even in the case of a weak skin effect. Under this condition Z has a simple form

$$Z = R_c - j(2\pi\omega/c^2)(d_m/2b) l \mu_e, \quad R_c = \tfrac{1}{2}\, b d_c \sigma_c, \tag{2}$$

where l is the film length, b is the width of the magnetic layers, d_m is the thickness of each magnetic layer, $2d_c$ is the cross section size of the conductive layer, σ_c and σ_m are the conductivities of the conductive layer and of the magnetic layer, and μ_e is the effective permeability of magnetic layers in the transverse direction. Expression (2) shows that the contribution of the magnetic layers to the sandwich impedance is described by the external inductance with respect to the inner layer,[20] and the external inductance has a linear dependence on μ_e. In this case, an obvious impedance change can be obtained at frequencies lower than those required for a single ferromagnetic layer.

In this paper, the results of GMI effects in FeCuNbSiB single layer and sandwiched films are presented, and the annealing influence and domain structures are also discussed. In sandwiched structures, FeCuNbSiB is used as outer ferromagnetic layers and Cu is employed as an inner layer. It is well known that FeCuNiSiB has excellent soft magnetic properties, such as very high permeability (as high as 10^5 at 1 kHz in the ribbon), low coercive force, and magnetostric-

tive contants.[21] The soft magnetic properties are related to the formation of fine bcc Fe crystallites, which have a mean diameter of 10–20 nm and are embedded in a residual amorphous phase, particularly after annealing at a suitable temperature. Cu is a material with high conductivity. It is expected that samples made by these materials will show large GMI effect.

EXPERIMENTAL DETAILS

The samples were fabricated using radio frequency (rf) sputtering equipment which has three targets. The FeCuNbSiB target is a disk made of a sintered alloy with a nominal composition of $Fe_{73.5}Cu_1Nb_3Si_{13.5}B_9$. Another target is a pure Cu disk. The targets and substrate holder were all water-cooled. The base vacuum was 5×10^{-6} Torr, 99.999% pure Ar gas was introduced and controlled at a pressure of 5×10^{-3} Torr during sputtering. The target surface was cleaned by presputtering for 2 h before deposition. The films were deposited onto Si substrates. The deposition rates were 0.05 and 0.14 nm/s for $Fe_{73.5}Cu_1Nb_3Si_{13.5}B_9$ and Cu, respectively. The single-layer samples were about 6.2 μm in thickness and were cut into 15 mm long and 3 mm wide for impedance measurements. The sandwiched films have a structure of F(3 μm)/Cu(1 μm)/F(3 μm) which is denoted as FCF, where F stands for FeCuNbSiB and C for Cu. The Cu layer with two electrodes at both ends is 0.3 mm wide and 15 mm long, while the F layers are 3 mm wide and 10 mm long. The shape of each layer was determined by a mask on the substrate. The single-layer films were annealed in a vacuum chamber (about 1×10^{-5} Torr) at 320, 360, 380, and 400 °C for 20 min, respectively, and the sample FCF was annealed in the same system at 250 °C for 2 h.

The GMI of the samples was measured at room temperature using an HP 4192A impedance analyzer, with a frequency range from 5 Hz to 13 MHz. The exposed parts of the Cu leads at both ends of sandwiched film were connected to the analyzer by an accessory 16048 B test lead. The measurements were carried out in the frequency range from 100 kHz to 13 MHz with a constant ac current amplitude of 10 mA and the probe current flew along the long direction of the samples. A pair of Helmholtz coils (30 cm in diameter) was used to generate a dc magnetic field ranging from -70 to 70 Oe. The coils were so placed that the magnetic field is perpendicular to the earth's magnetic field. In our experiments, we have studied GMI effects of the samples in longitudinal (the magnetic field is along the ac current direction) and transverse (the magnetic field is perpendicular to the ac current in the film plane) cases, respectively. The domain images were obtained by a digitally enchanced magneto-optical microscopy.[22] The experiments were arranged as follows: the sample was first magnetized to saturation along the sample long direction (longitudinally magnetized) or along the sample width direction (transversely magnetized), then the magnetizing field was decreased to zero, increased reversely to the coercive force of the sample, and then the field was decreased to zero. After that, the domain image was observed by the microscopy.

RESULTS AND DISCUSSION

From our observation, as-deposited single-layer films have no measurable MI effects. Annealing process releases the stress in the films and improves the soft magnetic properties. The results of MI and permeability μ_e measurements for the samples annealed at different temperatures showed that 380 °C is an optimum annealing temperature, so we will focus our attention only on the films annealed at 380 °C. Figure 1 shows the domain structure of annealed sample in longitudinally magnetized case. First, the domains consist of wide stripes and the orientation of them declines from the long direction of the sample. This indicates that there is an inclined anisotropy in the film, which consists of the stress-induced anisotropy and shape anisotropy. Figure 1 also shows that the anisotropy is uniform and there is no dispersion in the film. This anisotropy will affect GMI effect as discussed later. Second, many small and orderly arranged reversal domains distribute homogeneously in the film. The average size of these small domains is about 20 nm. Obviously, these single domains belong to the Fe nanocrystal particles, which are homogeneously embedded in the amorphous matrix. Therefore, the film is in the nanocrystalline state.

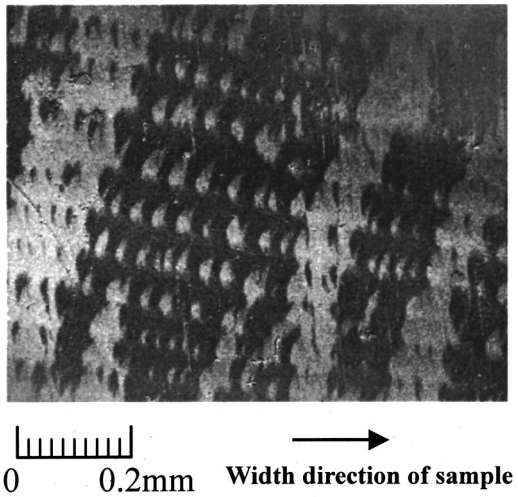

FIG. 1. Longitudinally magnetized domain structure of single layer FeCuNbSiB film annealed at 380 °C. The horizontal direction is the width direction of the sample.

Figure 2 shows the GMI dependences of a single layer film on the applied magnetic field at a frequency of 13 MHz for longitudinally (abbreviated as LMI) and transversely (abbreviated as TMI) magnetized cases, respectively. The MI ratio is expressed by $[Z(H)-Z(H_{\max})]/Z(H_{\max})$, where $Z(H)$ and $Z(H_{\max})$ are the impedances of the film at magnetic fields H and $H_{\max}$, respectively, and we use $H=70$ Oe as $H_{\max}$. We only give the results obtained in a positive field in Fig. 2. Similar results can be obtained when the magnetic field is negative, i.e., the MI curves are symmetric with respect to the magnetic field and are nonhysteresis. This is a usual feature of MI obtained in amorphous wires and ribbons.[5,15] Both the longitudinal and transverse MI spectra show a peak located at about 1 and 10 Oe, respectively. This result is different from that obtained by Sommer and Chien[17] in amorphous $Fe_{73.5}Cu_1Nb_3Si_{13.5}B_9$ films made by magnetron sputtering and then annealed in a transverse magnetic field, in which only the longitudinal MI spectrum has peaks, while the transverse MI spectrum is a single bell-shaped curve. Following the results obtained by

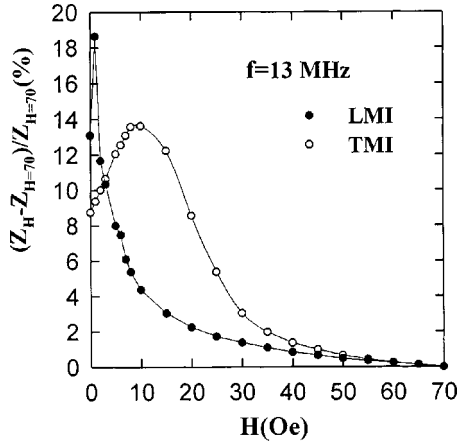

FIG. 2. Longitudinal (dots) and transverse (circles) magnetoimpedance ratio versus dc magnetic field at $f=13$ MHz. The impedance ratio is expressed as $[Z(H)\text{-}Z(H_{max})]/Z(H_{max})$, where $H_{max}=70$ Oe.

Sommer and Chien[17] in which only the transverse component of the magnetic anisotropy contributes to the longitudinal MI, a conclusion can be made from our results that the easy axis of the film must make an angle with the long film direction. The transverse and longitudinal components of the anisotropy contribute to the peaks on the MI curves. The anisotropies of the film include stress-induced and shape anisotropies. Zero-field annealing did not eliminate the stress-induced anisotropy as observed in Fe-based soft magnetic films[17] and ribbons.[6] This perhaps relates to the positive magnetostriction in Fe-based soft magnetic materials. The domain structure in Fig. 1 also confirms the existence of anisotropy in the film.

Figure 3 shows the dependences of LMI ratio (dots) and TMI ratio (circles), $[Z(0)-Z(H_{max})]/Z(H_{max})$, for the single layer film on the frequency f of the ac current, where $Z(0)$ is the film impedance at zero field, $H_{max}=70$ Oe. In the longitudinal case, the curve slope increases until at about 4 MHz, and then reaches to an almost constant after $f>4$ MHz. Similar behavior is observed for the transverse case. The GMI effect with negative curvature was usually observed in amorphous wires and ribbons at lower frequencies. It has been proved that the MI effects become significant only when the skin depth becomes smaller than the film thickness, so increasing the thickness of films can produce a larger MI effect at lower frequencies.

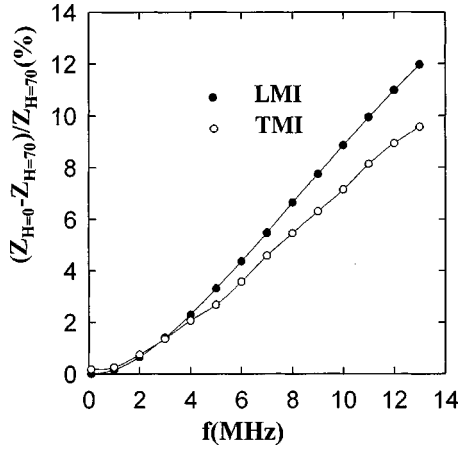

FIG. 3. The frequency dependences of LMI ratio (dots) and TMI ratio (circles), $[Z(0)\text{-}Z(H_{max})]/Z(H_{max})$, where $H_{max}=70$ Oe.

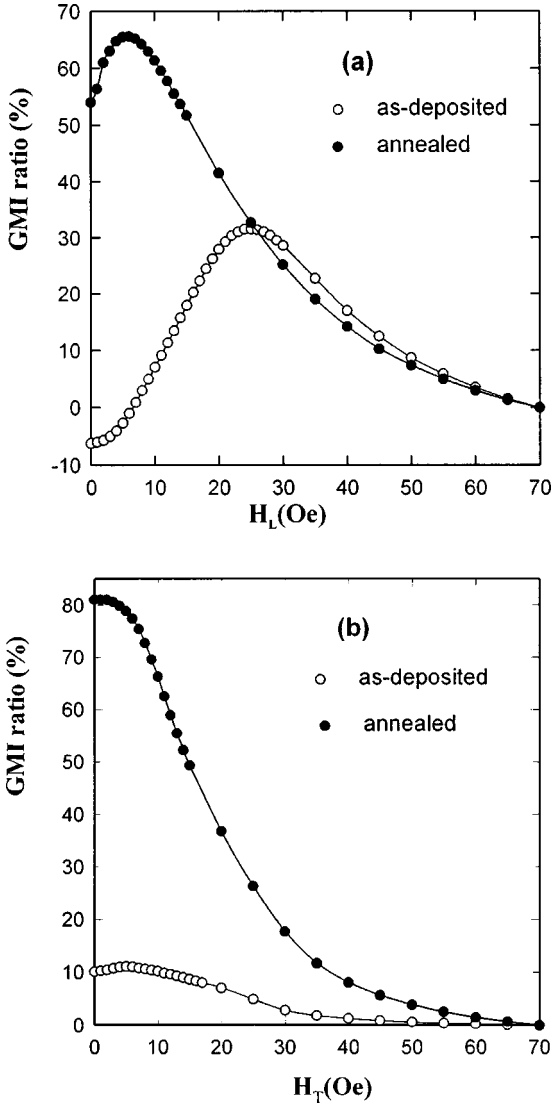

FIG. 4. The dependence of the GMI ratio of FeCuNbSiB/Cu/FeCuNbSiB on (a) longitudinal and (b) transverse applied magnetic fields at $f=13$ MHz.

Figures 4(a) and 4(b) show the dependence of GMI ratios of sandwiched films, FCF, on the longitudinal (a) and transverse (b) applied magnetic field at 13 MHz, respectively. The GMI ratio is defined as $\Delta Z/Z(H_{max})=[Z(H)-Z(H_{max})]/Z(H_{max})$, where $H_{max}=70$ Oe. The dots represent the results of annealed sample and the circles are for those of the as-deposited sample. We only give the results obtained in positive field in Fig. 4. Similar results can be obtained when the magnetic field is negative. An obvious feature for the sandwiched film is that large GMI effects are obtained in longitudinal and transverse cases even for the as-deposited samples, while almost no GMI effect can be detected for as-deposited single-layer films. This is an important advantage for sandwiched structure. It can be seen from Fig. 4(a) that the LMI ratio of the as-deposited sample first increases with the applied magnetic field from a very small value until reaching its maximum of 32% at about 25 Oe and then decreases as we further increase the applied field. The LMI

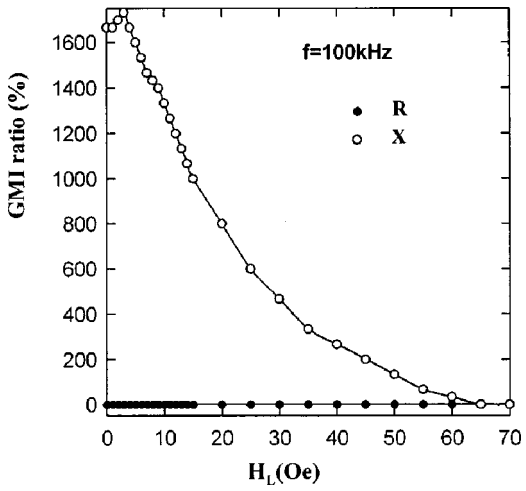

FIG. 5. Dependence of magnetoinductive and magnetoresistive ratios of FeCuNbSiB/Cu/FeCuNbSiB on the longitudinal applied magnetic field at $f = 100$ kHz.

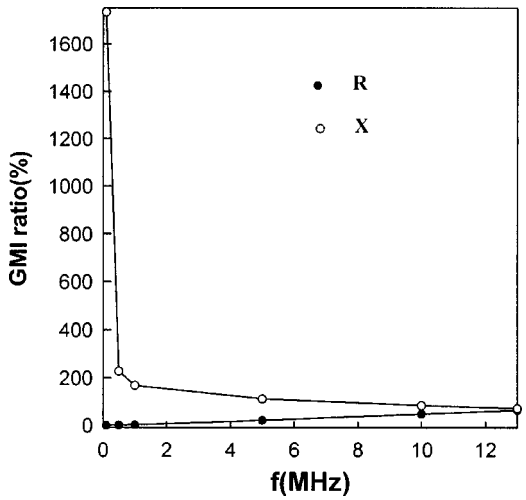

FIG. 6. Dependence of maximum magnetoinductive and magnetoresistive ratios of FeCuNbSiB/Cu/FeCuNbSiB versus frequency.

ratios of the annealed sample are much higher than those of as-deposited sample, especially in the low-field region. The maximum LMI ratio for the annealed sample is about 67% at about 6 Oe. It is much larger than that obtained in single-layer films. Its related peak is much smaller than that of the as-deposited sample. This indicates that the transverse anisotropy field in the annealed sample is much smaller than that of the as-deposited sample. The annealing process releases some stress in the sample induced during sputtering, and then reduces the anisotropy induced by the stress. We can also see from Fig. 4(a) that a 70-Oe magnetic field is not high enough to saturate the LMI effect.

In the transverse case, there is no obvious peak as seen in Fig. 4(b). This is different from the single-layer films. This is perhaps related to the closed ac magnetic flux loop in the magnetic layers. The maximum GMI ratios are 11% and 80% for as-deposited and annealed samples, respectively. The annealing process obviously improves the transverse GMI effect. Comparing Fig. 4(b) with Fig. 4(a), one can see that the transverse GMI ratio for annealed sample has a larger maximum value than that in longitudinal case and saturates easier. Comparing with single-layer films, one can conclude that the sandwiched structures possess obvious advantage in magnetoimpedance effect.

Another obvious feature of sandwiched structure is that the film shows a very large magnetoinductance effect at low frequencies. As we can see from Eq. (2), the applied magnetic field will reduce the value of μ_e, and the inductance component of Z will decrease linearly. At low frequencies, the magnetic film has a large μ_e, so the influence of field on μ_e is serious. When the frequency increases, μ_e decreases monotonously because of the influence of eddy current in the magnetic layers. So the relative change of μ_e in the field will be small at high frequencies. Figure 5 shows the dependence of inductive and resistive ratios on the longitudinal magnetic field at 100 kHz. Here the magnetoinductive and magnetoresistive ratios are defined as $[X(H)-X(H_{\max})]/X(H_{\max})$ and $(R(H)-R(H_{\max}))/R(H_{\max})$, respectively. The maximum change ratio of inductance is as large as 1733% at 100 kHz, while the resistance has no clear change in the entire range of applied magnetic field. The change of inductance decreases with increasing frequency because of the increase of eddy current loss in the magnetic layers, while the change of resistance will increase with increasing frequency because of the influence of skin effect. The maximum inductive and resistive change ratios versus frequency are shown in Fig. 6. Here the maximum magnetoinductive and magnetoresistive ratios are defined as $[X_{\max}-X(H_{\max})]/X(H_{\max})$ and $[R_{\max}-R(H_{\max})]/R(H_{\max})$, and $X_{\max}$ and $R_{\max}$ are the maximum values of X and R, respectively. The magnetoinductance decreases rapidly below 1 MHz, and then decreases slowly with increasing the frequency. While the magnetoresistance increases almost linearly with increasing frequency. At 13 MHz, the change of resistance is almost equal to that of inductance. This gives evidence that at lower frequencies, the giant magnetoinductance effect is dominant, while at higher frequencies, the change of resistance component gives the main contribution to GMI effects.

In order to know the dependence of GMI on the magnetic properties of the sandwiched films, we observed the domain structures of the film. Figures 7(a)–7(c) show the domain structures for as-deposited FCF sample, where (a) was taken from the center of a longitudinally magnetized sample, (b) was taken from the edge of this sample, and (c) was taken from the center of a transversely magnetized sample. From Figs. 7(a)–7(c), one can see the long and thin stripe domain patterns. The stripe easy axis declines towards the width direction of the sample. This is induced by an oblique anisotropy field. The transverse component of this anisotropy produces a peak of GMI ratio at about 25 Oe in Fig. 4(a) for the as-deposited sample. One can see from Fig. 7(b) that near the edge of sample, the orientation of domain changes towards the transverse direction and an increase in the number of the edge domains is clearly seen. This indicates that the easy axis near the sample edge is along the transverse direction, and the transverse demagnetizing and stray field at the edge make the increase of the domain number.[23] We can also see from Figs. 7(a)–7(c) that the domains are not uniform. This is caused by the stress inhomogeneity and defects in the sample. Figures 7(d)–7(f) show the domain structure for annealed FCF sample, where (d) was taken from the center of a longitudinally magnetized sample, (e) from the edge of this

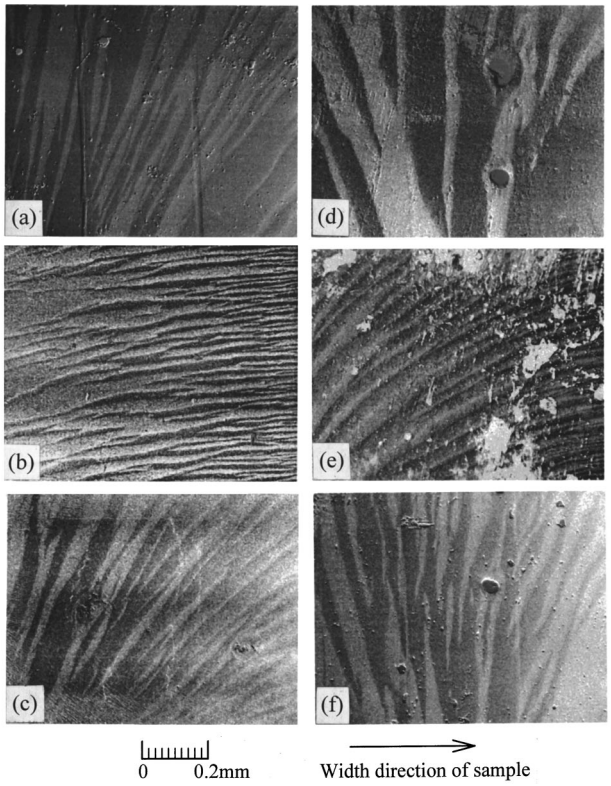

FIG. 7. Domain structures observed in longitudinally or transversely magnetized field for as-deposited [(a), (b), (c)] and annealed [(d), (e), (f)] sandwiched samples.

sample, and (f) from the center of a transversely magnetized sample. One can see from Fig. 7(d) that the domains are much wider than those for as-deposited sample. Although the domain orientations have some dispersion, the average orientation of the wide stripe domains is directed towards the long direction of the sample. The annealing process releases most of the stress in the sample, so the anisotropy induced by stress reduces obviously. The demagnetizing field makes the domain arrange towards the long direction of the sample. Near the edges of sample, the domain orientation changes gradually towards the transverse direction as seen in Fig. 7(e). The peak at about 6 Oe in Fig. 4(a) for the annealed sample is induced by the anisotropy dispersion in the film.

The average domain width in Fig. 7(d) is much larger than that observed in Fig. 7(f). This is because that in the longitudinally magnetizing process (along the easy axis direction), the magnetization is mainly caused by the reverse domain nucleation and domain wall displacement, but in the transverse magnetizing process (along the hard axis direction), the magnetization is mainly caused by the rotation of magnetic moments. In the transverse magnetizing process, the moments separately rotate to the opposite direction of the sample when the magnetizing field decreases to zero. Figure 7 indicates that the domain structures are not uniform in the as-deposited sample as well as the annealed sample. Therefore, the soft magnetic properties of the sample should not be the best ones because of the influence of the remaining stress in the sample. If the film can be annealed at a higher optimum temperature, the soft magnetic properties of sample will improve remarkably, and a better GMI effect can be obtained. Further work is being done in our laboratory.

In summary, large GMI effects are clearly seen in FeCuNbSiB single-layer and sandwiched films. This indicates that the Fe-based nanocrystalline FeCuNbSiB films are suitable for the GMI effect. Comparing with the single-layer films, the sandwiched structure has obvious advantages as follows: (1) The GMI effects are much larger than those in single layer films. Large GMI effects can be obtained even for the as-deposited sandwiched films, but no obvious GMI effects can be detected in the as-deposited single layer films. (2) The transverse GMI effects is better than the longitudinal one for sandwiched films, but a reverse case is obtained in single-layer films. This is associated with the closed ac magnetic flux loop in the transverse direction, and the influence of demagnetization effect for the ac magnetic field is also very weak. (3) The field dependence of permeability linearly determines the GMI effect in sandwiched films. In this case the impedance change can be large even at lower frequencies of a weak skin effect. Therefore, the skin effect is not essential. (4) A very large magnetoinductance effect (as large as 1733% at 100 kHz in our case) can be obtained at low frequencies in sandwiched films. (5) The GMI effects are closely related to the domain structure. The domain orientation determines the field position of GMI peak. The transverse arrangement of domains near the sandwiched film edge is favorable to the closed magnetic flux loop. This is one reason that a large GMI effect was obtained.

ACKNOWLEDGMENTS

The domain observations were done in the research group of R. Schäfer, IFW Dresden, Germany. This work was supported by the National Natural Science Foundation of China and the Research Fund for the Doctoral Program of Higher Education.

[1] K. Mohri, T. Kohzawa, K. Kawashima, H. Yoshida, and L. V. Panina, IEEE Trans. Magn. **28**, 3150 (1992).
[2] K. Kawashima, T. Kohzawa, H. Yoshida, and K. Mohri, IEEE Trans. Magn. **29**, 3168 (1993).
[3] L. V. Panina and K. Mohri, Appl. Phys. Lett. **65**, 1189 (1994).
[4] K. Mohri, K. Kawashima, T. Kohzawa, and Yoshida, IEEE Trans. Magn. **29**, 1245 (1993).
[5] L. V. Panina, K. Mohri, T. Uchiyama, K. Bushida, and M. Noda, IEEE Trans. Magn. **31**, 1249 (1995).
[6] C. Chen, K. Z. Luan, Y. H. Liu, L. M. Mei, H. Q. Guo, B. G. Shen, and J. G. Zhao, Phys. Rev. B **54**, 6092 (1996).
[7] M. Knobel, M. L. Sánchez, C. Gómez-Polo, P. Marin, M. Vázquez, and A. Hernando, J. Appl. Phys. **79**, 1646 (1996).
[8] Y. Ueda, S. Ikeda, and W. Takakura, J. Appl. Phys. **81**, 5787 (1997).
[9] G. V. Kurlyanddskaya, J. M. García-Beneytez, M. Vázquez, J. P. Sinnecker, V. A. Lukshina, and A. P. Potapov, J. Appl. Phys. **83**, 6581 (1998).
[10] Y. H. Liu, C. Chen, L. Zhang, S. S. Yan, and L. M. Mei, J. Phys. D **29**, 2943 (1996).

[11] S. Q. Xiao, Y. H. Liu, L. Zhang, C. Chen, J. X. Lou, S. X. Zhou, and G. D. Liu, J. Phys.: Condens. Matter **10**, 3651 (1998).
[12] K. Hika, L. V. Panina, and K. Mohri, IEEE Trans. Magn. **32**, 4594 (1996).
[13] L. V. Panina, K. Mohri, and T. Uchiyama, Physica A **241**, 429 (1997).
[14] A. Antonov, S. Gadetsky, A. Granovsky, A. D'yatckov, M. Sedova, N. Perov, N. Usov, T. Furmanova, and A. Lagar'kov, Physica A **241**, 414 (1997).
[15] L. V. Panina, K. Mohri, K. Bushida, and M. Noda, J. Appl. Phys. **76**, 6198 (1994).
[16] K. Mohri, Mater. Sci. Eng., A **185**, 141 (1995).
[17] R. L. Sommer and C. L. Chien, Appl. Phys. Lett. **67**, 3346 (1995).
[18] L. D. Landau and E. M. Lifshitz, *Electrodynamics of Continuous Media* (Pergamon Press, Oxford, 1975), p. 195.
[19] C. Kittel, Phys. Rev. **70**, 281 (1946).
[20] A. Paton, J. Appl. Phys. **42**, 5868 (1971).
[21] Y. Yoshizawa, S. Oguma, and K. Yamanchi, J. Appl. Phys. **64**, 6044 (1988).
[22] R. Schäfer, J. Magn. Magn. Mater. **148**, 226 (1995).
[23] R. Kolano, M. Kuzmiński, W. Gawior, and N. Wójcik, J. Magn. Magn. Mater. **133**, 321 (1994).